Chemical Science

RSC Publishing

EDGE ARTICLE

View Article Online
View Journal | View Issue

Cite this: *Chem. Sci.*, 2013, **4**, 1970

Ultra-sensitive chemosensors for Fe(III) and explosives based on highly fluorescent oligofluoranthene†

Xin-Gui Li,‡*[a] Yaozu Liao,‡[ab] Mei-Rong Huang,*[a] Veronica Strong[b] and Richard B. Kaner*[b]

Received 29th November 2012
Accepted 10th January 2013

DOI: 10.1039/c3sc22107e

www.rsc.org/chemicalscience

Electron-rich oligofluoranthene has been successfully synthesized by a one-step direct chemical oxidative oligomerization of fluoranthene. Key advantages include easy synthesis, high synthetic yield and low cost when compared with electropolymerization. Oligofluoranthene in solution is a very strong cyan fluorescence emitter with 12.2 times higher intensity than the fluoranthene monomer. The strong fluorescence can be effectively quenched by specific electron-deficient species, enabling the fabrication of low-cost, high-performance chemosensors for the selective detection of Fe(III) ions and the explosive 2,4,6-trinitrophenol (picric acid). A concentration range of >9 orders of magnitude with exceedingly low detection limits down to 10^{-12} M is possible. No sample enrichment is needed likely due to the synergistic effects of well-distributed π-conjugated electrons with a conical stereo configuration that may enhance the detection ability. Common interferents appear to have little effect as Fe(III) can be selectively detected in both tap water and seawater containing many other metal ions and picric acid can be detected at low concentrations even in the presence of inorganic acids.

Introduction

Conjugated aromatic compounds and polymers that demonstrate extensive π-electron delocalization and strong fluorescence emission have proven to be efficient fluorescent sensing materials which can be developed into amplified chemosensory systems.[1–3] Among these, an amplifying fluorescent polymer (AFP) is one in which all fluorophore units are quenched by a target analyte *via* transport of electronic excited states along the 1D molecular chains of the conjugated polymer. Unfortunately, this amplified quenching can be hindered by the strong self-quenching that arises from interchain interactions among polymer chains, in particular, when neighboring chains assemble parallel to each other. The formation of excimer-like states that results from π-stacking of an AFP can also reduce the sensory performance by providing traps that restrict the mobility of the excitons.[1] Therefore, the molecular design strategy of most AFPs has been based on 1D conjugated polymers possessing rigid scaffolds appended to the chains in order to suppress their strong interchain interactions including π–π stacking.[1,4,5] This also enhances adsorption and diffusion of analytes to favor their contact with fluorophore units.[6,7] Nevertheless, the synthesis of this kind of polymer is not without difficulties. The fluorescent polymers which often contain bulky side groups as well as receptors for specific analytes often require sophisticated multi-step synthetic techniques to produce.[1,2,8,9] Furthermore, for a 1D conjugated polymer with high molecular weight, an exciton is not able to visit the entire length along the high molecular weight chains due to its limited mobility and finite lifetime, even though the polymer can possess widely distributed electrons throughout the entire chains.[1,10] Because of these limitations, there is a need to develop new sensing materials that efficiently prevent π–π stacking between the fluorophore units and thus simply enable the maximum amplification for quenching to be realized.

Oligofluoranthene (OFA), a new small band gap conjugated oligomer, possesses novel electronic, optical, and photovoltaic properties due to its highly delocalized π-electrons.[11] OFA is believed to possess better optoelectronic properties and much higher thermal stability than the fluoranthene (FA) monomer due to increased delocalization of its π-conjugated electrons. However, due to its 1-D molecular chain structure and strong π–π stacking, the fluorescence emission from electro-synthesized OFA, like polypyrene, is not strong enough to fabricate chemosensors having ultra-high sensitivity.[12,13] The chemical oxidative synthesis of OFA has been problematic due

[a]*Institute of Materials Chemistry, Key Laboratory of Advanced Civil Engineering Materials, College of Materials Science and Engineering, Tongji University, 1239 Si-Ping Road, Shanghai 200092, China. E-mail: adamxgli@yahoo.com; huangmeirong@tongji.edu.cn; Fax: +86-21-65983871; Tel: +86-21-69582104*

[b]*Department of Chemistry & Biochemistry and California NanoSystems Institute, University of California, Los Angeles, California 90095, USA. E-mail: kaner@chem.ucla.edu; Fax: +1 (310) 825-5490; Tel: +1 (310) 825-5346*

† Electronic supplementary information (ESI) available: ^{1}H-NMR and MALDI-MS of FA and OFA, orbital electron distribution of the metal ions, UV-vis absorption spectra of OFA solution upon addition of Fe^{III} with different concentrations, comparison of the OFA fluorescent chemosensor with other ones for sensing Fe^{III}. See DOI: 10.1039/c3sc22107e

‡ X.-G. Li and Y.Z. Liao contributed equally to this work.

to the difficulty in controlling the chemical oxidative reaction, and up until now no high yield synthesis of strongly fluorescent OFA has been accomplished.

Here we explore a relatively simple one-step chemical oxidative oligomerization of fluoranthene (FA) in nitromethane using $FeCl_3$ as the oxidant to synthesize a novel form of OFA having a regular molecular structure, cone topology, and highly delocalized π-electrons. An optimized 3-D conic OFA structure could effectively hinder π–π stacking and aggregation that frequently occur in 2-D planar monomer molecules and 1-D linear polymers. This, in turn, could suppress π-electron transfer between fluorophores and thus avoid self-quenching of the conjugated oligomers. Additionally, the OFA structure would have an unusual electron-concentrative molecular effect, which may significantly enhance the electron donating power of the molecules to electron-deficient analytes. Therefore, a strongly amplifying effect to fluorescence emission and quenching could be possible in an OFA sensing system and the high efficiency of fluorescence quenching could enable sensing trace amounts of analytes even without a specific receptor. A new strategy for designing and synthesizing the molecular architecture of a merged fluorophore and receptor fluorescent sensor system is proposed and achieved with a simple, low-cost, scalable procedure. This opens up the possibility of fabricating advanced chemosensors that might find applications in ultra-sensitive, highly selective Fe^{III} and explosive sensors.

Experimental section

Materials

Fluoranthene (FA), anhydrous ferric chloride ($FeCl_3$), picric acid (PA), nitromethane (CH_3NO_2), amorphous non-fluorescent thermoplastic polysulfone (PSF) beads ($M_n \sim 22\,000$ by MO, autoignition temperature 1022 °F, melt index 6.5 g/10 min (343 °C/2.16 kg, ASTM D1238), hardness 69 (Rockwell M, ASTM D 785), refractive index n 20/D 1.633, reduced viscosity ~0.45 dL g^{-1}, T_g 190 °C, from Sigma-Aldrich) and other chemicals were of analytical grade and used as received.

Oligomerization procedure

As a typical procedure for the chemical oxidative oligomerization of FA, 1 mmol (0.21 g) of fluoranthene monomer and 5 mmol (0.81 g) of anhydrous $FeCl_3$ oxidant were separately dissolved in 5 mL of CH_3NO_2. The two solutions were kept in a 50 °C water bath for 30 min and then the $FeCl_3$ solution was slowly added into the monomer solution with magnetic stirring. The mixture was further stirred for 15 h at 50 °C. Upon adding one drop of oxidant solution into the monomer solution, the light-yellow monomer solution quickly turned orange. The color gradually became darker as more oxidant solution was added and eventually turned black. As-synthesized virgin oligo-fluoranthene (OFA) was obtained after a careful purification with ethanol and DI water by centrifugation in order to remove residual unreacted FA monomer and smaller oligomers that are soluble in ethanol. Dedoped pure Fe^{III}-free OFA was obtained by further thoroughly washing with 1.0 M HCl, 1.0 M NaOH and DI water several times at 50 °C, and then dried at 80 °C for 48 h, giving an oligomerization yield of 68.5%. Elemental analysis indicated that the C/H/N weight percentage in the OFA is 94.17/3.91/0.06%, respectively, signifying that the C/H molar ratio in the OFA is 2.01.

Preparation of an OFA/PSF composite film

A free-standing, robust, transparent OFA/PSF composite film was prepared by the following technique: 5 mg of OFA and 650 mg of PSF were dissolved in 7.0 g of NMP at 25 °C for the preparation of an 8.56 wt% OFA/PSF blend solution. This solution was cast onto a glass plate and heated at 65 °C for 20 h to remove the NMP to form a composite film containing 0.76 wt % OFA. Note that the solubility of the OFA in NMP and DMSO that are atypical solvents for polycyclic aromatics is quite good because stable homogeneous OFA solutions, uniform transparent OFA/PSF composite films, high-resolution ^{13}C-NMR and UV-vis spectra have been obtained, as shown in Fig. 1a, 3, 4b, and 6d.

Measurements

UV-vis spectra of fluoranthene monomer and dedoped OFA in NMP were recorded on a Perkin-Elmer Lambda 25 UV-vis spectrophotometer. ATR-FT-IR spectra were obtained with a Nicolet Magna-IRTM 550. Elemental analysis was performed by Columbia Analytical Services, Inc. USA. ^{1}H-NMR spectra were obtained using a Bruker ARX-400 and 500 MHz spectrometer with DMSO-d_6 as solvent. Wide-angle X-ray diffraction patterns were scanned on a Philips X'pert Pro powder diffractometer using copper-monochromatized CuKα radiation ($\lambda = 0.154178$ nm). Molecular weight of the soluble part of the OFA in DMSO as solvent was determined with 2,5-dihydroxybenzoic acid as the matrix on a matrix-assisted laser desorption ionization-time of flight mass spectrometer (MALDI-TOF MS) using a Voyager DE. Fluorescence spectra of fluoranthene and OFA in NMP and an OFA/polysulfone composite film were acquired on a QM-6SE

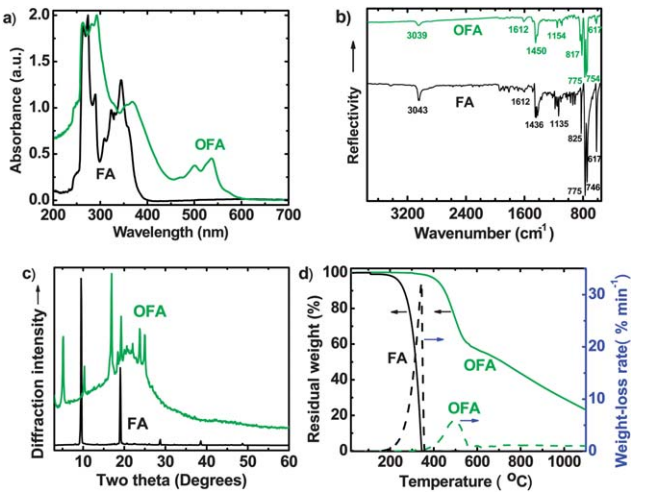

Fig. 1 (a) UV-vis and (b) ATR-FT-IR spectra; (c) wide-angle X-ray powder diffraction patterns, and (d) TGA and DTG of FA monomer and OFA oligomer synthesized with a $FeCl_3$/FA molar ratio of 5 : 1.

PTI fluorescence spectrometer. Fluorescent emission quenching experiments were carried out by sequentially adding 200 μL of Fe^{III} salt, PA, or an inorganic acid aqueous solution to 3 mL of an OFA solution (10 mg L^{-1}). Milli-Q water with resistivity of 18.2 MΩ cm was used for the preparation of all aqueous solutions. Two types of environmental water, *i.e.* tap water and seawater containing many metal ions served as real samples to examine the practical applicability of an OFA solution as an Fe^{III} chemosensor. The real water samples were filtered three times to completely remove any suspended solids and sediments before being added into 3 mL of an OFA solution (10 mg L^{-1}) for fluorescent emission quenching experiments in order to analyze the concentration of Fe^{III} in tap water and seawater samples by creating a calibration curve. The concentration of various metal ions in the real water samples was simultaneously analyzed by TJA RADIAL IRIS 1000 inductively coupled plasma-mass spectrometry (ICP-MS). Thermogravimetric analysis (TGA) was performed on a Perkin Elmer TGA Pyris 1 in argon at a heating rate of 15 °C min^{-1} between room temperature and 1100 °C. The bulk electrical conductivity of an approximately 0.5 mm thick pressed disk of the OFA particles was measured using a two-probe method with a useful area of 0.785 cm^2 at ambient temperature. Five replicates were run for every measurement and the relative standard deviation (RSD) for the various measurements was less than 2%.

Results and discussion

Synthesis and structure of OFA

Oligofluoranthene (OFA) has been synthesized for the first time by a facile one-step chemical oxidative oligomerization of FA in CH_3NO_2, as shown in Scheme 1. Compared with the insulating crystalline FA monomer, the OFA synthesized under an optimal $FeCl_3$ oxidant/FA monomer molar ratio of 5 : 1 for 15 h at 50 °C,

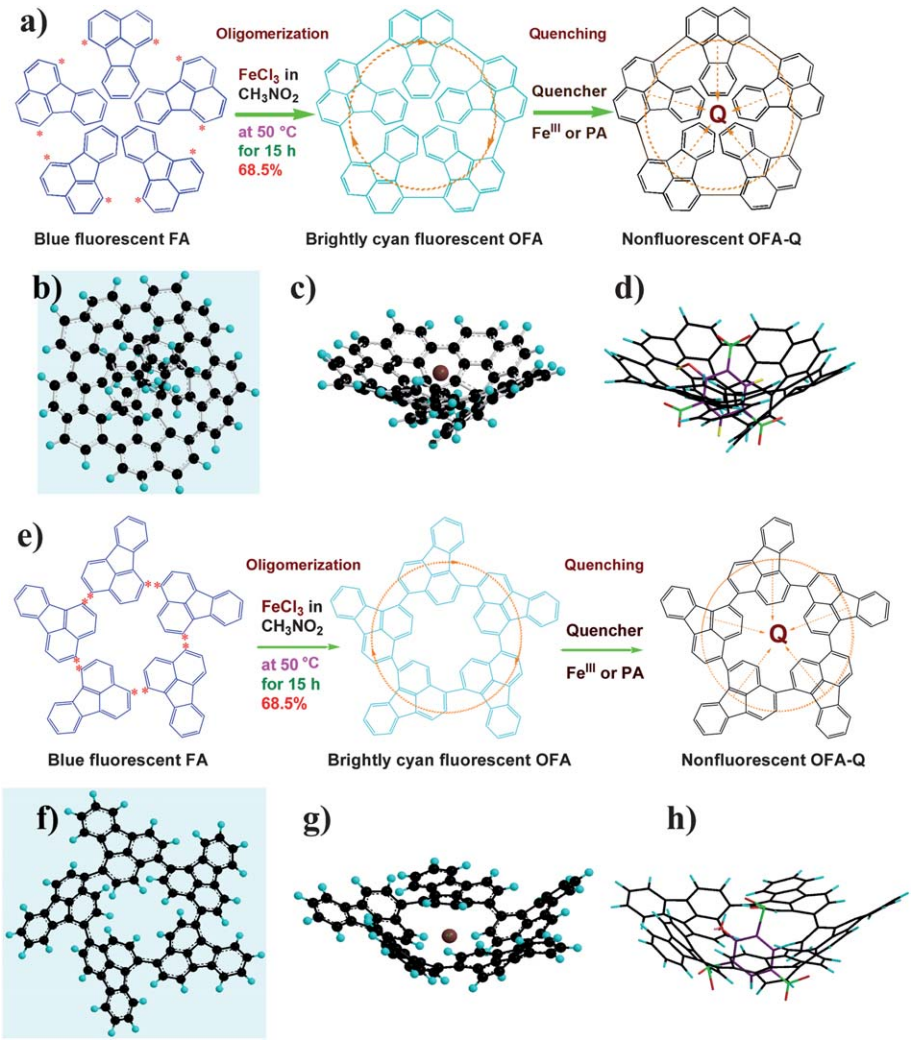

Scheme 1 (a) Symmetric and (e) asymmetric chemical oxidative oligomerizations of FA by (a) 1,6- and (e) 1,4-oxidative coupling could produce a conical shaped OFA with minimal energy as determined by Chem3D® Ultra Molecular Modeling and Analysis 2003. A schematic of the π-electron transfer complex with a quencher Q is presented where the orange dotted lines represent the π-electrons; a top view of the ball and stick model of the (b) symmetric and (f) asymmetric OFA; a side view of the ball and stick model of the (c) symmetric and (g) asymmetric OFA with Fe^{III} depicted as the bigger scarlet ball; and a side view of the stick model of the (d) symmetric and (h) asymmetric OFA–PA complex. The ball and stick models were created using Chem3D® Ultra Molecular Modeling and Analysis 2003 in order to show possible spatial configurations of the OFA.

demonstrates (1) additional and characteristic UV-vis absorbance bands at 501 and 537 nm due to its extensively delocalized π-conjugation (Fig. 1a); (2) a significantly different ATR-FT-IR spectrum having much weaker absorptions around 825 and 3039 cm^{-1} due to less out-of-plane bending and stretching modes (γ_{Ar-H}) due to some Ar–H bonds that disappear after oxidative dehydrogenation oligomerization (Fig. 1b), no OH and C=O characteristic absorptions in the IR spectrum that indicate no oxidation of the aromatic rings; (3) a C/H molar ratio of 2.01 based on elemental analysis; (4) a semicrystalline supramolecular structure (Fig. 1c) displaying six strong and moderate diffraction peaks at 5.20°, 10.31°, 16.93°, 19.23°, 23.75°, and 24.95°, while crystalline FA monomer displays only two strong diffraction peaks at 9.51° and 19.03°; (5) electrical semiconductivity of 1.02 × 10^{-4} S cm^{-1}, while FA monomer is an electrical insulator (conductivity < 10^{-8} S cm^{-1}); (6) a relatively high thermal decomposition temperature, high char yield at 1100 °C, and a slow weight-loss rate (Fig. 1d); (7) significantly different ^{1}H-NMR (Fig. S1†) and ^{1}H–^{1}H 2D COSY spectra (Fig. 2); (8) a remarkably broad ^{13}C-NMR spectrum exhibiting more resonance peaks (Fig. 3); (9) much weaker solubility in organic solvents; and (10) a dark red color, whereas FA monomer is light yellow. All of these strongly indicate oxidative dehydrogenating oligomerization of FA leading to the formation of OFA, the molecular structure of which has been characterized in detail as described below.

There are five cross peaks in the ^{1}H–^{1}H 2D COSY spectrum of OFA (Fig. 2b) rather than three cross peaks in FA (Fig. 2a). The cross peak (8.13, 7.72 ppm) of the FA monomer indicates a correlation between 1 and 2 (and 6 and 5), the cross peak (7.97, 7.72 ppm) indicates a correlation between 3 and 2 (and 4 and 5), and the cross peak (8.06, 7.43 ppm) indicates a correlation between 7 and 8 (and 9 and 10). For OFA, the cross peak (7.95, 7.70 ppm) due to the correlation between 3 and 2 (and 4 and 5) and the cross peak (8.09, 7.48 ppm) due to the correlation between 7 and 8 (and 10 and 9) suggest that a symmetric oxidative coupling of FA has occurred at positions 1 and 6. The cross peak (8.29, 7.85 ppm) due to the correlation between 1′ and 2′ (and 6′ and 5′) and the cross peak (8.20, 7.64 ppm) due to the correlation between 7′ and 8′ (and 10′ and 9′) suggest that another symmetric oxidative coupling of FA has occurred at positions 3′ and 4′. An additional cross peak at very close chemical shifts (7.62, 7.54 ppm) due to the correlation between 8″ and 9″ suggests that an asymmetric oxidative coupling of FA also has occurred at positions 1 and 4. As a result, three oxidative coupling modes between FA rings coexist during the oxidation oligomerization, forming three types of isomeric OFAs, as illustrated in Table 1. That is, the product obtained by this oxidation oligomerization is a mixture of symmetric and asymmetric oligomers. However, their conic configurations appear to be similar, as demonstrated in Scheme 1c, d, g, and h; therefore, the optimized result is a unique conic conjugated system containing concentrated π-electrons in the center. ^{13}C-NMR spectra of the FA monomer and OFA (Fig. 3) confirm the formation of wholly new carbons at 1′, 6′, 3′ and 4′ in the 1′,6′-, 3′,4′- and 1′,4′-bisubstituted FA units because of the oxidative coupling oligomerization. Additionally, a MALDI-TOF mass spectrum of OFA (Fig. S2†) indicates that the OFA is made up of 5 FA units (Table S1†) as the main population of cyclic oligomers. The linear and smaller oligomers may be attributed to the degradation products of the cyclic oligomers by the laser beam,[14] because these smaller oligomers consisting of 1–4 FA units have been completely removed during the post purification procedure. The removal of unreacted FA monomer and smaller oligomers from the resulting OFA products has been confirmed by four experimental facts: (1) no broad and/or gradually declining UV-vis absorbance corresponding to a mixture of FA monomer and 2–4 FA-units-containing oligomers having four types of different and gradually changing UV-vis absorbance characteristics was observed in the wavelength range from around 300 to 540 nm in the UV-vis spectrum of the resulting OFA products in Fig. 1a; (2) no sharp crystalline peaks corresponding to FA monomer were observed in the wide-angle X-ray powder diffraction pattern of the resulting OFA products in Fig. 1c; (3) no four-step gradual broad weight loss at relatively low temperature corresponding to a mixture of FA monomer and 2–4 FA-units-containing oligomers having four types of different and gradually increasing thermostability was found in the TG and DTG curves of the resulting OFA products in Fig. 1d; (4) a C/H molar ratio of 2.01 was indicated by elemental analysis. Therefore, one can deduce that the OFA is a five FA-units-containing cyclic oligomer likely with large π-conjugated cones as represented in Scheme 1.

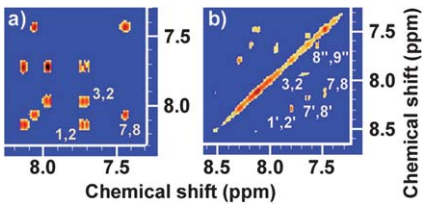

Fig. 2 500 MHz homonuclear correlated regular (^{1}H–^{1}H 2D COSY) spectra of (a) FA monomer and (b) OFA synthesized with a $FeCl_3$/FA molar ratio of 5 : 1.

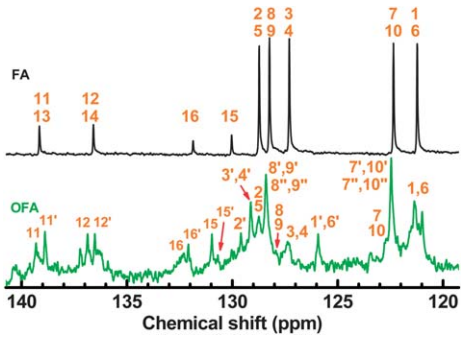

Fig. 3 500 MHz ^{13}C-NMR spectra of FA monomer and OFA synthesized with a $FeCl_3$/FA molar ratio of 5 : 1.

Strong fluorescence of OFA

Surprisingly, 10 mg L^{-1} of OFA in NMP solution emits 12.2 times stronger cyan fluorescence than FA under identical conditions including using the same FA concentration of 10 mg L^{-1} (Fig. 4a)

Table 1 ^{1}H and ^{13}C-NMR chemical shift assignments for FA monomer and OFA oligomer synthesized with a $FeCl_3$/FA molar ratio of 5 : 1

Fluoranthene (FA)			Oligofluoranthene (OFA)		
No.	^{1}H shift, ppm	^{13}C shift, ppm	No.	^{1}H shift, ppm	^{13}C shift, ppm
1	8.13	121.2	1/1′	−/8.29	125.9/121.4
2	7.72	128.7	2/2′	7.70/7.85	128.6/129.6
3	7.97	127.3	3/3′	7.95/−	127.4/129.1
4	7.97	127.3	4/4′	7.95/−	127.4/129.1
5	7.72	128.7	5/5′	7.70/7.85	128.6/129.6
6	8.13	121.2	6/6′	−/8.29	125.9/121.4
7	8.06	122.3	7/7′/7″	8.09/8.20/8.17	122.7/122.5/122.5
8	7.43	128.2	8/8′/8″	7.48/7.64/7.62	127.9/128.4/128.4
9	7.43	128.2	9/9′/9″	7.48/7.64/7.54	127.9/128.4/128.4
10	8.06	122.3	10/10′/10″	8.09/8.20/7.67	122.7/122.5/122.5
11	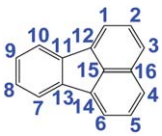	139.2	11/11′	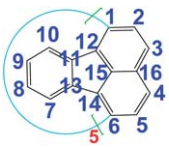	139.3/138.9
12		136.6	12/12′		136.8/136.5
13		139.2	13/13′		139.3/138.9
14		136.6	14/14′	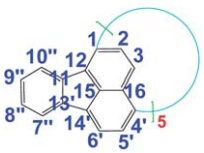	136.8/136.5
15		130.0	15/15′		131.0/130.8
16		131.9	16/16′	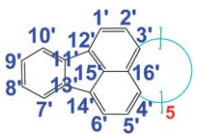	132.3/132.1

with the same spectrofluorometer and the same operational parameters including the identical slit width, under the respective optimal excitation wavelength of FA and OFA, while electrosynthesized OFA, in which the monomer repeat units are connected together two-dimensionally to give a planar architecture, emits only ~2 times stronger fluorescence than FA.[13] Furthermore, the excitation wavelength of 395 nm in OFA is longer than the 365 nm observed in fluoranthene monomer, implying that the energy of excitation in OFA is lower relative to the monomer. Besides the OFA solution, a free-standing robust composite film containing 0.76 wt% OFA in a non-fluorescent polysulfone (PSF) matrix emits very strong white light upon exposure to 365 nm UV light (Fig. 4c) despite its transparent orange color in sunlight (Fig. 4b). Compared with the OFA solution, the composite film displays a different fluorescence emission spectrum with longer wavelength and higher intensity at 550–650 nm (Fig. 4a), leading to white light, while the OFA solution emits bright cyan light.

The much stronger emission of OFA than FA can likely be attributed to a synergistic effect between the extended π-conjugated electrons and the optimized 3D conic architecture. Since, the structure can avoid close π–π stacking of fluorophores that can drastically depress fluorescence emission, the cone-like configuration would thus restrict the parallel face-to-face intermolecular interactions that limit fluorescence emission in both solution and solid OFA, as well as in solid OFA/polysulfone composite films. The bright white light from the film could potentially be used in selectively sensitive fluorescent probes,[3,15] organic light-emitting diodes,[16] organic photovoltaics[16] and possibly fluorescent falsification-resistant inks, while the remarkably enhanced emission from the OFA solution prompted us to fabricate ultra-sensitive fluorescent chemosensors with a wide linear detection range and extremely low detection limits.

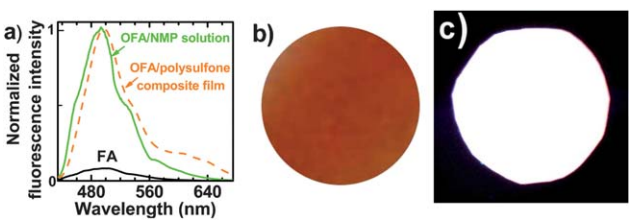

Fig. 4 (a) Fluorescent emission spectra of the FA monomer, an OFA solution in NMP and an OFA/polysulfone composite film; (b) and (c) a free-standing transparent OFA/PSF composite film with a thickness of *ca.* 20 μm under (b) sunlight and (c) 365 nm UV light.

Ultra-sensitive fluorescent chemosensors

The emission fluorescence quenching of the OFA solution upon interaction with different metal ions at a concentration of

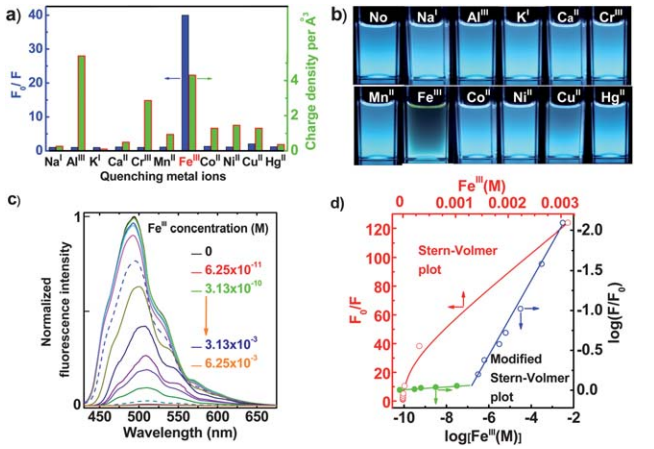

Fig. 5 Regular quenching of fluorescence emission excited (blue bar in a, c, d) at 395 nm and (b) at 365 nm of an OFA solution at 10 mg L^{-1} in NMP upon adding aqueous metal ions at a 3.13×10^{-4} M concentration; (green bar in a) charge density of the metal ions; (c) regular quenching upon adding 6.25×10^{-11} M to 6.25×10^{-3} M of Fe^{III}; (d) linear correlations between $\log(F/F_0)$ and $\log[Fe^{III}]$, *i.e.*, $\log(F/F_0) = 3.22 + 0.470 \log Fe^{III}$ in 10^{-7} to 10^{-2} M range and $\log(F/F_0) = 0.0846 + 0.0189 \log Fe^{III}$ in 10^{-11} to 10^{-7} M range. F_0 and F represent the fluorescence intensity of OFA solution without and with quencher, respectively, *i.e.*, F/F_0 is defined as the relative fluorescence intensity.

3.13×10^{-4} M is shown in Fig. 5a and b. Fe^{III} has a dramatic effect enhancing quenching fluorescence emission by 40 times. In other words, OFA is highly fluorescence sensitive and selective to Fe^{III} over the other ten common metal ions coexisting in the same aqueous solution. This may be due to the stronger electron-withdrawing ability of Fe^{III} that can be attributed to its relatively high charge density (Fig. 5a) that partially fills all the d orbitals (Scheme S1†), and higher standard electrode potential (Table S2†) when compared to the other metal ions examined. Al^{III} also has a high charge density, but it does not possess any partially filled outer d orbitals, and its standard electrode potential is low. Although Mn^{II} also has a complete set of partially filled outer d orbitals, its charge density and standard electrode potential are both relatively low. Note that Hg^{II} exhibits a low charge density and contains no partially filled outer d orbitals despite its high standard electrode potential. Therefore, among the metal ions studied, only Fe^{III} has the ability to effectively withdraw electrons from OFA, thus efficiently leading to the formation of a π-electron transfer complex with the OFA. This has been confirmed by the dependence of the UV-vis absorption of OFA around 374 nm on the Fe^{III} concentration (Fig. S3†). This high selectivity allows for the use of just one kind of sensor molecule rather than two or more[17] when distinguishing between a large numbers of metal ions.

While a Stern–Volmer plot for the OFA fluorescence quenching with Fe^{III} ions shows a downward curvature rather than linear behavior, a modified Stern–Volmer plot displays a linear correlation between the fluorescence quenching and the concentration of Fe^{III} ions added. Two linear correlation coefficients of 0.9963 and 0.9815 are found over a very extensive Fe^{III} concentration range between 6.25×10^{-11} M and 3.13×10^{-3} M as presented in Fig. 5c and d. The Stern–Volmer quenching process used here was chosen from among several modified Stern–Volmer linear fit methods.[18,19] Thus, it appears that this new "turn-off" chemosensor exhibits a very high sensitivity towards Fe^{III} even at exceedingly low concentrations down to 6.25×10^{-11} M in aqueous solution. This is 3–5 orders of magnitude better than AD-SRhB/β-CD-DNS supramolecular-complexes,[20] rhodamine-modified Fe_3O_4 nanoparticles,[21] and Alexa fluor 488 (ref. 22) for Fe^{III} detection in aqueous solution. It is also better than most other aromatic molecular chemosensors for the detection of Fe^{III} ions in buffers[23–26] or in organic solutions,[27–30] and better than most polymeric chemosensors,[31,32] while comparable to polyfluorenes,[33] as shown in Table S3.† This ultra-sensitive Fe^{III} sensor could be useful for many applications perhaps even for monitoring Fe^{III} concentrations in the food chain in the oceans.

Another electron-deficient compound, the explosive picric acid (PA), can quench the fluorescence of OFA with an even higher sensitivity. Note that PA was chosen for the purpose of evaluating explosive sensing because of its commercial availability, high explosive power equivalent to 105% of TNT (2,4,6-trinitrotoluene), and wide usage in industry where environmental contamination can present a problem due to its high solubility (Table 2). In fact, trace and ultra-trace explosive detection in the last decade has attracted much attention because of the globalization of terrorist acts, and due to water and soil contamination when used for military purposes.[34] Fig. 6a, b, c, and d show that PA in aqueous solution quenches the fluorescence emission of OFA quantitatively with high efficiency. The Stern–Volmer plot for the OFA fluorescence quenching with PA exhibits an upward curvature, but the modified Stern–Volmer plot displays a good linear correlation between the emission intensity and PA concentration with linear correlation coefficients of 0.9976 down to 5.00×10^{-4} M and 0.9989 down to a concentration of 1.00×10^{-12} M (Fig. 6a and b). Note that the modified Stern–Volmer equation for the fluorescence quenching with PA is different from that with Fe^{III} discussed above, because the Stern–Volmer plots of the fluorescence quenching with Fe^{III} and PA in Fig. 5d and 6b are reversed. This "turn-off" chemosensor possesses at least a 5 order of magnitude lower detection limit than Am-functionalized 1-ethynylpentaphenylsilole,[35] polymetallole,[36] polytrifluoropropylmethylsilane,[37] TPE-containing polytriazoles,[38] Eu^{3+}–TTA complex,[39] a nanoscopic

Table 2 Comparison between two typical explosives 2,4,6-trinitrophenol and 2,4,6-trinitrotoluene

Full name (abbreviation)	Appearance	Sensitivity to bump (%)	Sensitivity to friction (%)	Explosive speed (m s^{-1})	Energy released (MJ kg^{-1})	Solubility in water (g L^{-1})
2,4,6-Trinitrophenol (PA)	Pale yellow crystal	24–36	0	7350	4.52	14
2,4,6-Trinitrotoluene (TNT)	Pale yellow crystal	Lower	0 (≤353 N)	6900	4.20	0.130

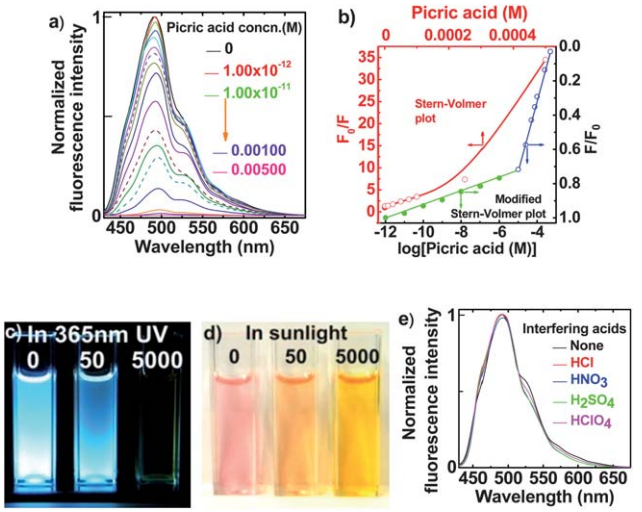

Fig. 6 (a) Regular quenching of the fluorescence emission excited at 395 nm of an OFA solution at 10 mg L^{-1} in NMP upon adding aqueous PA between 1.00 × 10^{-12} M to 5.00 × 10^{-3} M; (b) linear relationships between F/F_0 and the logarithm of the PA concentration, *i.e.*, $F/F_0 = 0.524 - 0.0405\log[PA]$ in 10^{-12} to 10^{-5} M range and $F/F_0 = -1.35 - 0.414$ log[PA] in 10^{-5} to 10^{-3} M range. An OFA solution at 10 mg L^{-1} upon adding 0, 50, and 5000 μM PA under (c) 365 nm UV and (d) sunlight; (e) fluorescence emission stability of the OFA solution containing 1.0 × 10^{-6} M PA upon adding 0.1 M HCl, HNO_3, H_2SO_4, and $HClO_4$ as interfering acids, respectively.

prism self-assembled by $Pt(PEt_3)_2(NO_3)$ triphenylamine,[40] a clip-type amide,[40] and phosphole oxide,[41] as summarized in Table S4.† Additionally, the present OFA chemosensor covers a wide linear detection range, up to 8 orders of magnitude, which compares favorably to the typical 1–3 orders of magnitude obtained with other common fluorescent chemosensors. Moreover, the fluorescent OFA chemosensor has excellent anti-interference ability towards four ordinary inorganic acids, even when the concentration of these interferents is as high as 0.1 M (Fig. 6e). To the best of our knowledge, the OFA chemosensor is currently one of the most easily prepared and most sensitive sensors for detecting picric acid.

Both calibration curves for Fe^{III} and PA show a two-section response behavior. Both slopes show a lower sensitivity in the dilute range than in the concentrated range (Fig. 5d and 6b), which arise from the small increase in the amount of absolute quenchers in the dilute interval compared to the large quencher concentration in the concentrated range. However, the relatively lower slope in the dilute section does not imply a weaker quenching efficiency. On the contrary, these two electron-deficient quenchers both possess high quenching efficiency, which can be calculated quantitatively. In the dilute range from 6.25 × 10^{-11} to 6.25 × 10^{-7} M of Fe^{III}, a classic Stern–Volmer equation: $F_0/F = 1.04 + 2.09 \times 10^6$ [Fe^{III}], $R = 0.9898$, can be fit, giving a very large association constant, 2.09 × 10^6 M^{-1}, for the OFA–Fe^{III} complex when compared to other chemosensors (Table S3†).This suggests a highly effective static quenching of Fe^{III} by the fluorescence emission of OFA. Similarly, a large association constant, 6.10 × 10^4 M^{-1} of the OFA–PA complex (Table S4†), also suggests a highly effective static quenching, in which the association constant was obtained according to the Stern–Volmer equation: $F_0/F = 0.960 + 6.10 \times 10^4$ [PA], $R = 0.9974$ over the whole detection range. Furthermore, the slope of the linear relationship in the lower quenching range is higher for detecting PA than Fe^{III} (Fig. 5d and 6b) because of an even high electron deficiency of PA relative to Fe^{III}, resulting in even stronger electron transfer from the OFA to the PA, which is likely responsible for the superior detection limit for PA. Besides its concentration, quite different linear slopes can be used to differentiate the existence of Fe^{III} from PA in unknown samples. For example, by diluting an unknown sample to create a series of samples with different concentrations, one can identify the species in the unknown sample based on the slope diversity of the quenching results of the OFA emission. This OFA chemosensor may also be useful for the analysis of Fe^{III} and PA coexisting in real samples as long as proper pretreatment is made to remove one of them in advance.

Strong fluorescence quenching in the presence of small molecule quenchers may result from an electron-transfer quenching effect, by which a non-fluorescent charge-transfer complex between the OFA and the quenchers is formed *via* electrostatically attractive interactions and electron transfer from the center of the OFA to the quencher molecules.[42,43] It should be appreciated that this is an amplified quenching in the OFA system, because one of the small molecule quenchers, Fe^{III} or PA, can quench five fluoranthene units at the same time rather than just one unit as in the monomer system. The binding of the quencher molecule produces a trapping site whereby the excitation of the OFA is effectively deactivated by electron transfer quenching. The excitation rapidly transfers energy to an exciton that can quickly migrate between iso-energetic sites around the highly π-conjugated OFA resulting in a low-energy acceptor site. Moreover, the low energy acceptor site has the ability to accept electrons from the excited state of the oligomer. This destroys the excited state of the conjugated OFA and effectively quenches its fluorescing properties. Therefore, binding one receptor site results in an efficient quenching of all emitting units in an entire OFA oligomer. This remarkable amplified effect, together with a possible stereo configuration that can readily capture electron-deficient species, may explain why such an ultra-sensitive fluorescence quenching, even at a very low concentration (6.25 × 10^{-11} M of Fe^{III} and 1.0 × 10^{-12} M PA), is possible.

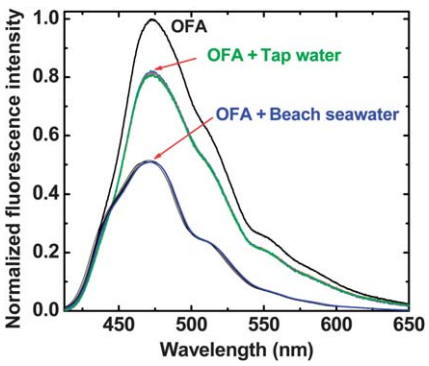

Fig. 7 Fluorescence quenching of OFA upon the addition of tap water and Santa Monica beach seawater both at (15 : 1, v/v).

Table 3 The determination of Fe^{III} concentration in real water samples by the OFA chemosensor *vs.* ICP-MS

Real sample	Other metal ion (μM)		[Fe^{III}] detected by ICP-MS (μM)	[Fe^{III}] detected by the OFA chemosensor (μM) 1/2/3/4/5/**average**	RSD (%)	Relative error (%)
Tap water	Pb^{II}	<0.1	3.44	3.49/3.50/3.49/3.54/3.58/**3.52**	1.12	2.23
	Hg^{II}	<0.1				
	Cd^{II}	<0.18				
	Cu^{II}	1.095				
	Zn^{II}	5.301				
	Ca^{II}	1071				
	Na^{I}	1683				
Santa Monica Beach water	Cd^{II}	0.367	8.24	9.59/9.58/9.45/9.40/9.18/**9.44**	1.77	14.6
	Ag^{I}	0.385				
	Ni^{II}	0.790				
	Co^{II}	0.828				
	Mn^{II}	0.936				
	Cr^{III}	1.18				
	Cu^{II}	1.19				
	Zn^{II}	2.46				
	Hg^{II}	11.5				
	K^{I}	11 400				
	Ca^{II}	13 900				
	Mg^{II}	58 200				
	Na^{I}	548 000				

Assay of real water samples

The OFA chemosensor has been used to analyze both tap water and seawater. Fluorescence spectra for a solution of OFA (10.0 mg L^{-1}) in NMP-water (15 : 1, v/v) after addition of pure water and actual seawater samples (Fig. 7) have been applied to give analytical results that are very close to those detected by traditional ICP-MS with only a small relative error (2.23–14.6%) as given in Table 3 regardless of the coexistence of other metal ions. As can be seen, the error is slightly higher for the analysis of seawater containing many more metal ions at much higher concentrations, but it is still well within the bounds of acceptability (15%). The fact that the OFA-based chemosensor possesses a highly selective response to Fe^{III} in mixed metal ions has thus been reconfirmed. Therefore, the present chemosensor could be useful for an accurate and selective analysis of Fe^{III} in real water samples, using a substantially less sophisticated experimental procedure than atomic absorption spectroscopy.

Conclusions

We have synthesized a unique electron-rich OFA with a conical molecular architecture and unusual electron-concentrative molecular effect by a one-step chemical oxidative oligomerization of FA. This method provides a number of key advantages including a high yield, low-cost synthesis, good thermal stability, and strong fluorescent emission, when compared to previously reported electropolymerization. The OFA structure can effectively hinder the π–π stacking of the fluorophores that in turn prevents self-quenching, thus endowing OFA with enhanced fluorescence emission and maximum quenching amplification. The strong fluorescence can be linearly and selectively quenched by electron deficient substances, such as the explosive picric acid, even at an ultra-trace level down to 10^{-12} M. The present chemosensor has been successful for an accurate and selective analysis of Fe^{III} in real samples including seawater containing 13 types of other metal ions at up to 630 mM. This investigation provides an alternative route to synthesize highly sensitive molecules in a straightforward and simple fashion. We believe that this study will stimulate further research on fluorescent sensor molecules for detecting electron-deficient substances using this new strategy of designing and synthesizing a molecular architecture where a fluorophore and a receptor are combined in a simple synthetic procedure.

Acknowledgements

The authors thank the National Natural Science Foundations of China (50873077 and 51273148, X.G.L. and 51203090, Y.Z.L.), the Natural Science Foundation of Shanghai (12ZR1446700, Y.Z.L.) and Abraxis Bioscience (R.B.K.) for financial support. The authors also acknowledge Dr Qihai Xu for the NMR measurements and Ms Yue Wang for the MS measurements.

Notes and references

1 S. W. Thomas III, G. D. Joly and T. M. Swager, *Chem. Rev.*, 2007, **107**, 1339–1386.
2 L. Basabe-Desmonts, D. N. Reinhoudt and M. Crego-Calama, *Chem. Soc. Rev.*, 2007, **36**, 993–1017.
3 J. S. Yang and T. M. Swager, *J. Am. Chem. Soc.*, 1998, **120**, 5321–5322.
4 H. Tan, M. Wang, C.-T. Yang, S. Pant, K. K. Bhakoo, S. Y. Wong, Z.-K. Chen, X. Li and J. Wang, *Chem.–Eur. J.*, 2011, **17**, 6696–6706.

5 L.-V. Mathieu, D. Brouard and D. Boudreau, *J. Phys. Chem. C*, 2011, **115**, 2974–2981.
6 P. H. Kwan, M. J. MacLachlan and T. M. Swager, *J. Am. Chem. Soc.*, 2004, **126**, 8638–8639.
7 H.-C. Chu, Y.-H. Lee, S.-J. Hsu, P.-J. Yang, A. Yabushita and H.-C. Lin, *J. Phys. Chem. B*, 2011, **115**, 8845–8852.
8 F. He, T. Gadt, I. Manners and M. A. Winnik, *J. Am. Chem. Soc.*, 2011, **133**, 9095–9103.
9 S. X. Deng, T. M. Fulghum, G. Krueger, D. Patton, J.-Y. Park and R. C. Advincula, *Chem.–Eur. J.*, 2011, **17**, 8929–8940.
10 M. S. Park, A. Aiyar, J. O. Park, E. Reichmanis and M. Srinivasarao, *J. Am. Chem. Soc.*, 2011, **133**, 7244–7247.
11 M. Kertesz and A. Ashertehrani, *Macromolecules*, 1996, **29**, 940–945.
12 X. G. Li, Y. W. Liu, M. R. Huang, S. Peng, L. Z. Gong and M. G. Moloney, *Chem.–Eur. J.*, 2010, **16**, 4803–4813.
13 J. Xu, J. Hou, S. Zhang, H. Y. Xia and S. Z. Pu, *J. Phys. Chem. B*, 2006, **110**, 2643–2648.
14 E. Girard, J.-D. Marty, B. Ameduri and M. Destarac, *ACS Macro Lett.*, 2012, **1**, 270–274.
15 K. Zhang, H. Zhou, Q. Mei, S. Wang, G. Guan, R. Liu, J. Zhang and Z. Zhang, *J. Am. Chem. Soc.*, 2011, **133**, 8424–8487.
16 T. M. Figueira-Duarte and K. Mullen, *Chem. Rev.*, 2011, **111**, 7260–7314.
17 S. S. Tan, S. J. Kim and E. T. Kool, *J. Am. Chem. Soc.*, 2011, **133**, 2664–2671.
18 X. B. Zhang, C. C. Guo, Z. Z. Li, G. L. Shen and R. Q. Yu, *Anal. Chem.*, 2002, **74**, 821–825.
19 J. Hong and L. M. Gierasch, *J. Am. Chem. Soc.*, 2010, **132**, 10445–10452.
20 M. Xu, S. Wu, F. Zeng and C. Yu, *Langmuir*, 2010, **26**, 4529–4534.
21 B. Wang, J. Hai, Z. Liu, Q. Wang, Z. Yang and S. Sun, *Angew. Chem., Int. Ed.*, 2010, **49**, 4576–4579.
22 J. P. Sumner and R. Kopelman, Nanosensors, *Analyst*, 2005, **130**, 528–533.
23 J. L. Bricks, A. Kovalchuk, C. Trieflinger, M. Nofz, M. Bueschel, A. I. Tolmachev, J. Daub and K. Rurack, *J. Am. Chem. Soc.*, 2005, **127**, 13522–13529.
24 T. Palanché, F. Marmolle, M. A. Abdallah, A. Shanzer and A.-M. Albrecht-Gary, *J. Biol. Inorg. Chem.*, 1999, **4**, 188–198.
25 N. Singh, N. Kaur, J. Dunn, M. MacKay and J. F. Callan, *Tetrahedron Lett.*, 2009, **50**, 953–956.
26 J. Mao, L. Wang, W. Dou, X. Tang, Y. Yan and W. Liu, *Org. Lett.*, 2007, **9**, 4567–4570.
27 M. H. Lee, T. V. Giap, S. H. Kim, Y. H. Lee, C. Kang and J. S. Kim, *Chem. Commun.*, 2010, **46**, 1407–1409.
28 J. Q. Wang, L. Huang, M. Xue, Y. Wang, L. Gao, J. H. Zhu and Z. G. Zou, *J. Phys. Chem. C*, 2008, **112**, 5014–5022.
29 N. Singh, N. Kaur and J. F. Callan, *J. Fluoresc.*, 2009, **19**, 649–654.
30 K. Sung, H. K. Fu and S. H. Hong, *J. Fluoresc.*, 2007, **17**, 383–389.
31 Y. Hu, B. Wang and Z. Su, *Polym. Int.*, 2008, **57**, 1343–1350.
32 N. J. Li, Q. F. Xu, X. W. Xia, L. H. Wang, J. M. Lu and X. W. Wen, *Mater. Chem. Phys.*, 2009, **114**, 339–343.
33 G. Zhou, G. Qian, L. Ma, Y. X. Cheng, Z. Y. Xie, L. X. Wang, X. B. Jing and F. S. Wang, *Macromolecules*, 2005, **38**, 5416–5424.
34 Y. Engel, R. Elnathan, A. Pevzner, G. Davidi, E. Flaxer and F. Patolsky, *Angew. Chem., Int. Ed.*, 2010, **49**, 6830–6835.
35 Z. Li, Y. Q. Dong, J. W. Y. Lam, J. X. Sun, A. J. Qin, M. Häußler, Y. P. Dong, H. H. Y. Sung, I. D. Williams, H. S. Kwok and B. Z. Tang, *Adv. Funct. Mater.*, 2009, **19**, 905–917.
36 H. Sohn, M. J. Sailor, D. Magde and W. C. Trogler, *J. Am. Chem. Soc.*, 2003, **125**, 3821–3830.
37 A. Saxena, M. Fujiki, R. Rai and G. Kwak, *Chem. Mater.*, 2005, **17**, 2181–2185.
38 A. Qin, J. W. Y. Lam, L. Tang, C. K. W. Jim, H. Zhao, J. Sun and B. Z. Tang, *Macromolecules*, 2009, **42**, 1421–1424.
39 J. Lu and Z. Zhang, *Anal. Chim. Acta*, 1996, **318**, 175–179.
40 S. Ghosh and P. S. Mukherjee, *Organometallics*, 2008, **27**, 316–319.
41 K. Shiraishi, T. Sanji and M. Tanaka, *ACS Appl. Mater. Interfaces*, 2009, **1**, 1379–1382.
42 L. J. Fan, Y. Zhang, C. B. Murphy, S. E. Angell, M. F. L. Parker, B. R. Flynn and W. E. Jones Jr, *Coord. Chem. Rev.*, 2009, **253**, 410–422.
43 D. T. McQuade, A. E. Pullen and T. M. Swager, *Chem. Rev.*, 2000, **100**, 2537–2574.

